NeuroImage **11,** 326–333 (2000)
doi:10.1006/nimg.2000.0549, available online at http://www.idealibrary.com on IDEAL®

A Study of Analysis Parameters That Influence the Sensitivity of Event-Related fMRI Analyses

Joseph B. Hopfinger,* Christian Büchel,† Andrew P. Holmes,‡ and Karl J. Friston†

*The Psychology Department and Center for Neuroscience, University of California, Davis, California 95616; †The Wellcome Department of Cognitive Neurology, Institute of Neurology, Queen Square, London WC1N 3BG United Kingdom; and ‡Robertson Centre for Biostatistics, Boyd Orr Building, University Avenue, Glasgow, G12 8QQ, Scotland, United Kingdom

Received October 1, 1999

To assess the effect of various analysis parameters on the sensitivity of event-related fMRI analyses, 36 analyses were performed on a single fMRI data-set, varying parameters along four axes: (1) resampled voxel size; (2) spatial smoothing; (3) temporal smoothing; and (4) the set of basis functions used to model event-related responses. Sensitivity (i.e., the probability of detecting an activation given it exists) was assessed in terms of *Z* scores and by a metric for corrected *P* values, the negative log of the expected Euler characteristic. Sixteen brain regions distributed across cortical and subcortical areas were included in the meta-analysis. Main effects on sensitivity were found for resampled voxel size, spatial smoothing, temporal smoothing, and the set of basis functions chosen. The analysis parameters that generally produced the most sensitive analyses were a 2-mm^3 resampled voxel size, 10-mm spatial smoothing, 4-s temporal smoothing, and a basis set comprising a hemodynamic response function and its temporal derivative.

INTRODUCTION

The analysis of fMRI data typically entails multiple stages of data preprocessing. Within each stage, specific values must be chosen for each processing parameter. The ideal choice is the value that renders the analysis most sensitive (in terms of the probability of detecting an activation given it exists), while conforming to the assumptions of the statistical model employed. The aim of this study was to test empirically four analysis parameters, in order to determine the effects that these choices may have on the sensitivity of the analysis. The present set of analyses were all performed as event-related analyses, however, only one of the parameters investigated, the set of basis functions chosen to model the hemodynamic response, relates solely to event-related designs. The other three analysis parameters are applicable to fMRI analyses in general. In this paper, we do not consider acquisition parameters. Rather, we are concerned exclusively with analysis parameters that determine data processing and statistical modeling after the data are acquired.

Regardless of the specific form of analysis, the brain volumes from fMRI time-series typically need to be realigned with each other (e.g., Thacker *et al.*, 1999) and may be normalized to a standard stereotactic space. During these stages, it is often necessary to resample the original images by interpolation methods in order to apply the spatial transformations (Friston *et al.*, 1995a). In relation to voxel size, it is possible to resample the data to reduce or increase voxel size. Although one does not create any further information, the format of the resampled data conforms more closely to a lattice representation and therefore enables the application of Gaussian field theory. Smaller voxel sizes ensure that the data conform to a good lattice representation and therefore reduce the likelihood that any of the assumptions required by the application of Gaussian field theory are violated. Here we tested how resampling the final volumes to either a resampled voxel size of 2 or 3 mm^3 would affect the sensitivity of the final analysis.[1] Smaller resampled voxel sizes allow the use of a smaller spatial filter and therefore are sometimes considered preferable for localization purposes. Here, however, we tested explicitly whether smaller resampled voxel sizes necessarily provide more sensitivity.

After the volumes have been realigned (and possibly normalized, as well), the images may be spatially smoothed, in order to increase signal relative to noise

[1] The correction for head-motion in the realignment stage and the transformation of the brain in the normalization stage, typically cause the volume data to be shifted out of the acquisition plane. Therefore resampling is required even when the desired resampled voxel size is the same as the original acquired voxel size.

1053-8119/00 $35.00

and to assure that the residual images conform to a lattice approximation of Gaussian random fields (to ensure the corrected inference is valid). Here, we smoothed the data with either a 6-, 10-, or 14-mm isotropic Gaussian kernel, to examine how spatial smoothing affects sensitivity of the ensuing analysis. Before performing statistical analyses, the data may also be temporally smoothed in order to assure the veracity of the assumed form for serial autocorrelations (e.g., Friston *et al.*, 1995b; Worsley and Friston, 1995; Zarahn *et al.*, 1997). This may be done by convolving the data with a Gaussian kernel approximating the hemodynamic response (but see also Purdon and Weisskoff, 1998, and Zarahn *et al.*, 1997, for alternative methods). As temporal smoothing is used here only to condition the autocorrelation structure to reduce bias in estimating the standard error (Friston *et al.*, submitted), it is not necessary for the smoothing kernel to have the identical shape as the hemodynamic response. Here, we tested two sizes of Gaussian convolution kernel: 4-s full-width at half maxima (FWHM) and 8-s FWHM.

Within the current study, we also examined one parameter space specific to event-related fMRI analysis techniques. As described previously (Josephs *et al.*, 1997; Friston *et al.*, 1998), it is possible to model event-related responses using a synthetic hemodynamic response function (HRF) that is a compound of basis functions of peristimulus time. Here, we tested three hierarchical sets of basis functions for the modeling of the fMRI data: (i) A synthetic hemodynamic response function (HRF) alone (modeled by the sum of two gamma functions—one to model the initial increase in perfusion with a peak latency of 6 s, a second to model the under-shoot on recovery with a latency of 16 s). (ii) The HRF with its partial derivative with respect to time (temporal derivative). (iii) The HRF with its partial derivative with respect to time and its partial derivative with respect to dispersion. Adding partial derivatives, according to a first-order Taylor approximation, allows the model to account for differences in timing (temporal derivative) and width (dispersion derivative) of the hemodynamic response. Here, we tested explicitly whether including these derivatives in the statistical model has a measurable effect on sensitivity.

In the meta-analysis described in this paper we focus on a single data-set acquired from a single subject and analyzed with a fixed-effects analysis. This ensures that the effects of analysis parameters are not confounded by interactions with intersubject variability (e.g., Aguirre *et al.*, 1998) or task-specific responses. We employed an activation paradigm that evoked responses in multiple cortical and subcortical areas that are assumed to represent canonical cortical and subcortical activations. Generalization to other task designs should not be a problematic issue in the sense that our goal was to assess the effects of various analysis parameters on the sensitivity of detecting activations in cortical and subcortical regions, irrespective of the particular task that caused them (see also Skudlarski *et al.*, 1999). The generalization to multisubject studies, however, must be qualified. The introduction of multiple subjects into the statistical model introduces a new source of variability that might interact with some of the analysis parameters that we have manipulated. For example, intersubject variability in functional anatomy may render increasing degrees of smoothing more appropriate for a sensitive analysis. This means that the effects of analysis parameters may differ between a fixed-effects analysis of a single subject and a random-effects analysis of multiple subjects. Having said this, however, the optimum parameters for a fixed-effects analysis are likely to be similar to those in a random-effects analysis because the most sensitive characterization is the most efficient, thereby decreasing the variance of the parameter estimates that enter into a second level or random-effects analysis. Furthermore, we chose to restrict our meta-analysis to a fixed-effects model because some of the parameters we explored are only meaningfully defined at the first or fixed-effects level (e.g., number of basis functions modeling evoked hemodynamic responses). A further meta-analysis of random-effect models that incorporates subject variability would represent an extension of the work described in this paper.

METHODS

The data came from a pilot study (one male subject, with informed consent and no neurological or psychiatric abnormalities), similar to a fMRI study of classical conditioning published previously (Büchel *et al.*, 1998). At the beginning of each trial, a face was presented at fixation for 3 s. One half of the faces were followed by a loud burst of white noise (100 dB) for 500 ms (conditioned face stimuli, CS+) and the other half were never followed by noise (Neutral). The intertrial interval between successive face stimuli was varied randomly between 10 and 14 s.

Data Acquisition

The data were acquired using a 2 Tesla Magnetom VISION (Siemens, Erlangen) MRI system. Contiguous multislice T2*-weighted images were obtained using a head volume coil, with a gradient echo-planar sequence

using axial slice orientation (TE = 40 ms, 80.7 ms/image, 64 × 64 pixels giving a 19.2 × 19.2 cm FOV, TR = 4.1 s, readout duration per line = 600 μs, total readout time = 38.4 ms, no apodization was done during image reconstruction). The brain was covered by 48 axial slices obtained with an in-plane resolution of 64 × 64, and 3-mm^3 isotropic voxels. The first 8 scans of each run were discarded to allow for T1 magnetic saturation effects. The remaining 316 volume images then comprised the time-series, which was analyzed. Bitemporal foam pressure pads were used to stabilize the subject's head.

Data Preprocessing

The data were analyzed with SPM97 (Wellcome Department of Cognitive Neurology). The time-series volume images were realigned and corrected for movement-related effects (the onset of the noise burst did not produce gross sudden movements by the subject, as measured by estimated head motion). The data were then spatially normalized to a standard stereotactic space (Talairach and Tournoux, 1988) using the subject's coregistered structural T1 scan (Friston *et al.*, 1995a). Statistical analyses were performed using the event-related method described previously (e.g., Josephs *et al.*, 1997; Friston *et al.*, 1998), with the specific analysis parameters described below.

Investigated Analysis Parameters

Resampled voxel size. At the normalization step, the volumes were resampled, by sinc interpolation, to either 2 or 3-mm^3 resampled voxels.

Spatial smoothing. The data were smoothed with a 6-, 10-, or 14-mm isotropic Gaussian kernel.

Temporal smoothing. Two sizes of Gaussian convolution kernel were compared: 4-s FWHM and 8-s FWHM.

Basis functions. Three hierarchical sets of basis functions were used for modeling of the fMRI data; a canonical hemodynamic response function (HRF) alone, the HRF with its temporal derivative, and the HRF with its temporal derivative and dispersion derivative.

All possible combinations of the analysis parameters listed above were used in a multifactorial design—resulting in the 36 analyses (2 × 3 × 2 × 3) that were used in the meta-analysis. The data were proportionately scaled to a grand mean of 100 arbitrary units to account for overall differences in intensity of whole brain volumes across the time series, and low-frequency confounds were modeled by a discrete-cosine high-pass "filter" set with a cut-off period of 97.64 s (Holmes *et al.*, 1997). Three events of interest were included in the statistical model: (1) visual presentation of conditioned faces (CS+); (2) visual presentation of neutral faces (NEUTRAL); and (3) auditory noise. The following four contrasts were then specified: (1) visual stimuli (conditioned and neutral faces) against baseline; (2) auditory stimuli (auditory noise) against baseline; (3) conditioned versus neutral faces; and (4) neutral versus conditioned faces. For all analyses presented here, only the basis functions representing the canonical HRF for each event of interest were given nonzero weightings in the contrast specification. Since it was not important for our purposes whether the temporal or dispersion derivatives were positive or negative, the parameter estimates for those basis func-

TABLE 1

Brain Regions Used for Meta-Analysis

Brain region	Stereotactic coordinates (mm) x, y, z	Contrast
1. Middle occipital gyrus (area 19)	19, −106, 14	Visual stimuli
2. Fusiform/lingual gyrus	−26, −85, −20	Visual stimuli
3. Area 8	46, 11, 26	Visual stimuli
4. Prefrontal cortex	50, 14, −7	Visual stimuli
5. Medial temporal cortex	66, −5, −3	Auditory stimuli
6. Superior temporal cortex	−57, −30, 10	Auditory stimuli
7. Thalamus*	9, −24, −7	CS+ > neutral
8. Insula	54, 14, −3	CS+ > neutral
9. Medial frontal/cingulate	3, 0, 58	CS+ > neutral
10. Cerebellum*	15, −59, −39	CS+ > neutral
11. Occipital/cuneus gyrus	11, −82, 31	CS+ > neutral
12. Medius frontal gyrus	52, 6, 46	CS+ > neutral
13. Hippocampus (Left)*	−24, −16, −28	Neutral > CS+
14. Frontal/prefrontal cortex	53, −6, 24	Neutral > CS+
15. Medial frontal	−10, 57, 15	Neutral > CS+
16. Hippocampus (Right)*	38, −25, −25	Neutral > CS+

Note. The visual and auditory contrasts are relative to baseline. CS+, conditioned visual stimuli (see text for details). Asterisks (*) denote subcortical regions. All other regions were considered cortical regions, for the factor of "Type of Brain Region" in the ANOVAs discussed in the text.

FIG. 1. Comparison of the effects of spatial smoothing on cortical versus subcortical brain regions. Region numbers listed across horizontal axes refer to the numbers listed in Table 1. (A) Plot of the uncorrected *Z* scores for each of the cortical regions tested here, as a function of spatial smoothing, showing a consistent decrease in sensitivity as the size of the spatial smoothing increases. (B) Plot of the uncorrected *Z* scores for each of the subcortical regions tested here, as a function of spatial smoothing. Subcortical regions did not show a decreasing sensitivity with increasing spatial smoothing, as cortical regions did, but rather showed higher sensitivity with the larger smoothing kernels of 10 and 14 mm.

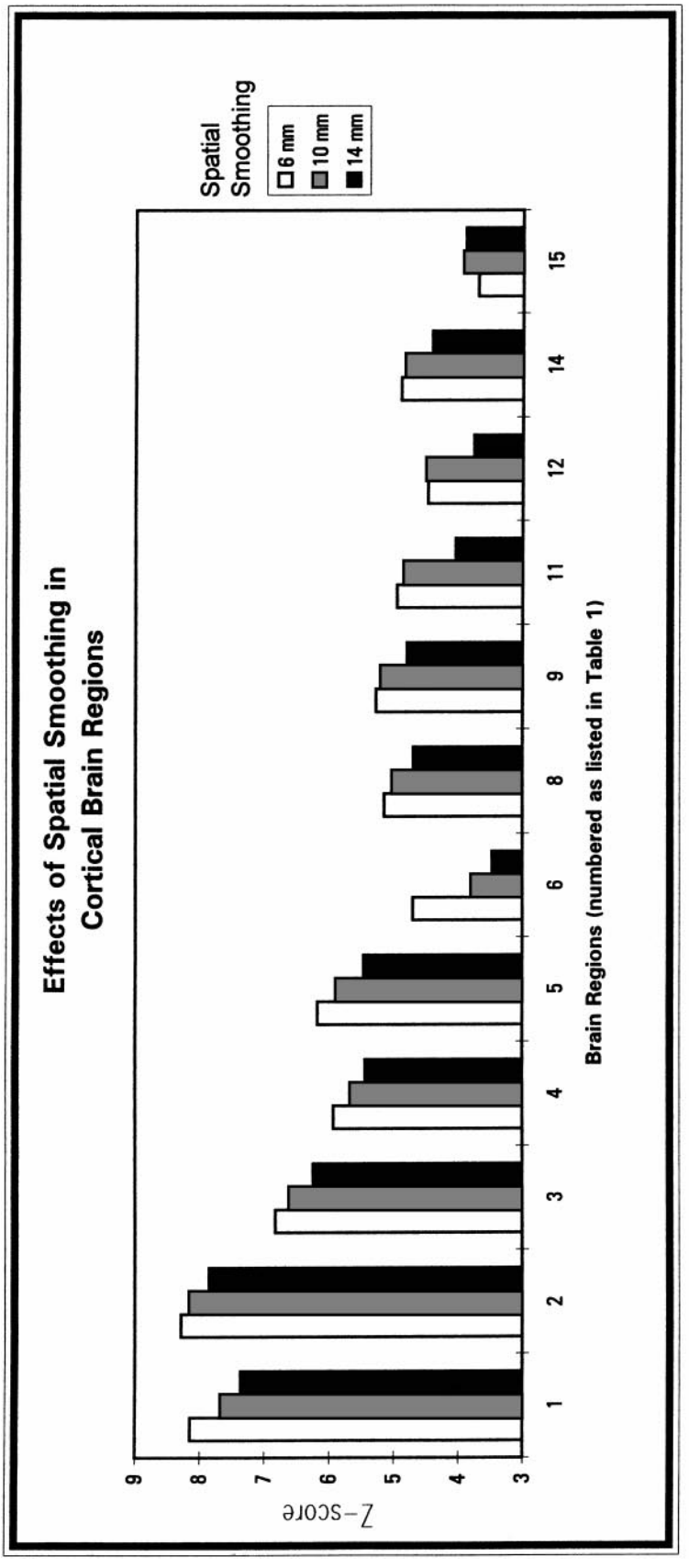
Effects of Spatial Smoothing in
Cortical Brain Regions
Spatial
Smoothing
6 mm
10 mm
14 mm
Z-score
9
8
7
6
5
4
3
1
2
3
4
5
6
8
9
11
12
14
15
Brain Regions (numbered as listed in Table 1)

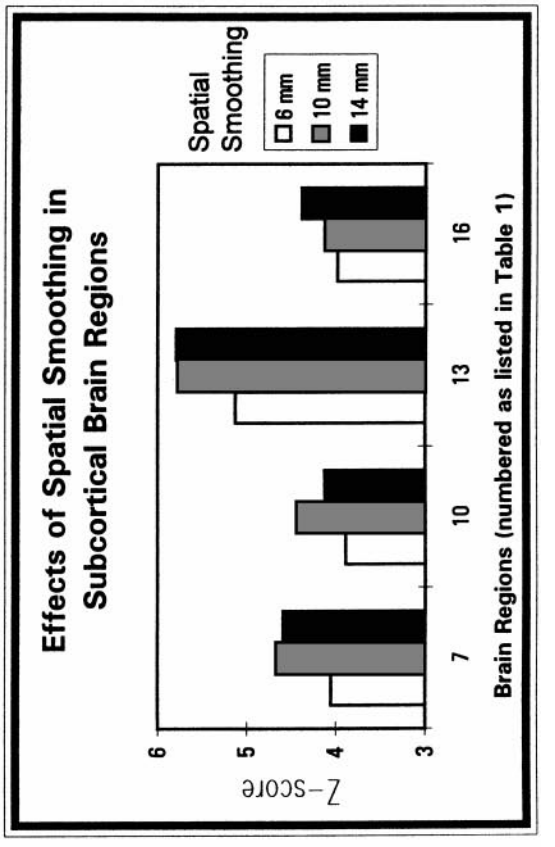
Effects of Spatial Smoothing in
Subcortical Brain Regions
Spatial
Smoothing
6 mm
10 mm
14 mm
Z-score
6
5
4
3
7
10
13
16
Brain Regions (numbered as listed in Table 1)

tions were not part of the specified contrasts (i.e., were given zero weightings in the contrasts). Rather, the basis functions representing those derivatives were used in the specified models only to account for the variance arising from those types of possible variability in the HRF response.

Using the SPM{*t*}s resulting from the four contrasts above, 16 brain regions were selected for inclusion in the meta-analysis. All sixteen regions evidenced suprathreshold voxels in all thirty-six analyses. Table 1 lists the 16 brain regions and the contrasts that revealed the activations. Sensitivity was measured by two metrics: (1) *Z* score; and (2) the negative natural log of the expected Euler characteristic corresponding to that *Z* score. The latter was used as a metric for *P* values after correction for multiple comparisons (see Adler, 1981, and Worsley, 1994, for a description of the Euler characteristic). It is important to include a statistic that reflects corrected inferences because the correction is a function of spatial smoothness. The effect of spatial smoothing can enter at two distinct levels in determining the sensitivity of an analysis. First, increasing the smoothness generally increases the sensitivity of the resulting SPMs by virtue of the matched filter theorem. This is a natural consequence of the fact that the spatial frequency of the noise is generally higher than signal in neuroimaging data. As a result, suppressing high frequency contributions with spatial smoothing increases the signal to noise ratio and the sensitivity of the analyses. The second way in which smoothing affects sensitivity is that it introduces spatial dependencies among the data that reduce the correction to the *P* values for the volume analyzed. Note that this effect is expressed only in terms of the corrected *P* value (but not the uncorrected *P* value).

Two separate ANOVAs were performed, one for sensitivity measured as *Z* scores (relating to the uncorrected *P* values), a second for sensitivity after correction for multiple comparisons (the metric based on the Euler characteristic). In cases where there exist strong *a priori* predictions about particular brain regions, the uncorrected scores are relevant. In cases where there are not strong a priori reasons to investigate a particular brain structure, the corrected scores are appropriate. Therefore, both are presented here, as either is fundamentally relevant, depending upon whether the inferences are to be made about a particular brain region or an effect that occurs anywhere in the search volume. Each of the mixed-design ANOVAs for the scores across the 16 brain regions included the within region factors of (1) Resampled voxel size (two levels), (2) Spatial smoothing (three levels), (3) Temporal smoothing (two levels), and (4) Set of basis functions (three levels); and included the between region factor of Type of Brain Region (two levels: cortical and subcortical, as noted in Table 1).

TABLE 2

Results of ANOVA for Uncorrected *Z* Scores

	Analysis of variance for *Z* scores				
Source	DF	SS	MS	F	*P*
Main effects					
Resampled voxel size	1	0.54	0.54	12.40	0.003*
Spatial smoothing	2	12.78	6.39	14.53	0.000*
Temporal smoothing	1	79.66	79.66	12.34	0.003*
Basis functions	2	17.80	8.90	5.09	0.013*
Type of brain region	1	81.66	81.66	1.40	0.257
2-way interactions					
Resampled voxel × spatial	2	0.06	0.03	0.55	0.583
Resampled voxel × temporal	1	0.02	0.02	1.75	0.207
Resampled voxel × basis	2	0.004	0.002	0.08	0.923
Resampled voxel × type	1	0.05	0.05	1.21	0.291
Spatial × temporal	2	0.17	0.09	0.59	0.559
Spatial × basis	4	0.04	0.01	0.14	0.966
Spatial × type	2	20.39	10.19	23.19	0.000*
Temporal × basis	2	0.79	0.40	0.65	0.528
Temporal × type	1	5.29	5.29	0.82	0.381
Basis × type	2	5.17	2.58	1.48	0.245

RESULTS

The ANOVA for sensitivity as measured by uncorrected *Z* scores revealed main effects of Resampled voxel Size, Spatial Smoothing, Temporal Smoothing, and Set of Basis Functions (see Table 2). Data with a resampled voxel size of 2 mm^3 produced greater sensitivity than with a resampled voxel size of 3 mm^3 (Table 4, middle column, presents the means of the uncorrected *Z* scores). Data spatially smoothed with either a 6- or 10-mm isotropic kernel produced more sensitive analyses than when a 14-mm kernel was used, and temporal smoothing with a 4-s FWHM kernel produced greater sensitivity than temporal smoothing with an 8-s FWHM kernel. Analyses that modeled the responses either with the hemodynamic response function (HRF) alone or the HRF with only the temporal derivative showed greater sensitivity than analyses that used the basis set consisting of the HRF with temporal and dispersion derivatives.

While there was no main effect of Type of Brain Region (cortical versus subcortical), there was a significant interaction between Type of Brain Region and Spatial Smoothing (Table 2). Specifically, except for two regions in the medial frontal lobes, the cortical regions showed a consistent decrease in sensitivity as the spatial smoothing increased (Fig. 1, top). However, the subcortical regions tested here did not show that trend (Fig. 1, bottom), and, in fact, the right and left hippocampal activations (13 and 16 in Fig. 1) showed the opposite

TABLE 3

Results of ANOVA for Corrected Scores

Source	Analysis of variance for corrected scores (−ln (Euler char.)) DF	SS	MS	F	*P*
Main effects					
Resampled voxel size	1	8.02	8.02	13.49	0.003*
Spatial smoothing	2	166.83	83.42	9.75	0.001*
Temporal smoothing	1	2286.67	2286.67	12.50	0.003*
Set of basis functions	2	493.40	246.70	5.11	0.013*
Type of brain region	1	2505.59	2505.59	1.35	0.264
2-way interactions					
Resampled voxel × spatial	2	1.21	0.61	0.86	0.433
Resampled voxel × temporal	1	0.06	0.06	0.40	0.536
Resampled voxel × basis	2	0.06	0.03	0.10	0.903
Resampled voxel × type	1	0.92	0.92	1.54	0.235
Spatial × temporal	2	1.19	0.59	0.21	0.810
Spatial × basis	4	2.99	0.75	0.44	0.776
Spatial × type	2	443.43	221.71	25.92	0.000*
Temporal × basis	2	0.35	0.18	0.01	0.989
Temporal × type	1	330.77	330.77	1.81	0.200
Basis × type	2	14.90	7.45	0.15	0.858

trend of increasing *Z* scores with increasing degrees of spatial smoothing.[2] There were no other significant two or three-way interactions.

When sensitivity was assessed using corrected values, main effects were again found for Resampled voxel Size, Spatial Smoothing, Temporal Smoothing, and Set of Basis Functions (see Table 3). Similar to the uncorrected scores, a resampled voxel size of 2 mm^3 again produced higher sensitivity than a 3 mm^3 resampled voxel size, temporal smoothing with a 4-s kernel produced higher sensitivity than smoothing with an 8-s kernel, and modeling the data with the HRF alone or with the temporal derivative resulted in more sensitive analyses than when the dispersion derivative was included (Table 4, right column, presents the means of the corrected scores). However, as might be expected, the direction of the effect of spatial smoothing was different for the corrected scores than it was for the uncorrected scores. While a spatial smoothing of 6 mm produced the highest sensitivity when measured by uncorrected scores, a spatial smoothing of 6 mm gave the lowest sensitivity as measured by corrected scores. For the corrected scores, a spatial smoothing of 10 mm yielded the highest sensitivity. Similar to the uncorrected scores, there was no main effect of Type of Brain Region for the corrected scores, but there was again a significant 2-way interaction between Type of Brain Region and Spatial Smoothing. Specifically, subcortical regions showed increasing sensitivity with increasing size of the spatial smoothing kernel, while the largest smoothing kernel produced the least sensitive analyses for cortical regions. No other two or three-way interactions were significant in the analysis of the corrected scores.

[2] One possible explanation for this difference is that subcortical regions may show a slightly different hemodynamic response. In addition to showing an opposite pattern to the cortical regions in terms of spatial smoothing, the hippocampal regions also showed a trend toward higher sensitivity with an 8-s temporal smoothing. This was in contrast to all other regions (except for one superior temporal region) that showed a lower sensitivity with the 8-s temporal smoothing. The differences noticed here may highlight the need to examine the HRF individually in different brain regions, especially in subcortical regions where the neural architecture differs from that in the surrounding cortex. Indeed, Rajapakse *et al.* (1999) suggest that the hemodynamic response depends on a number of factors, including the neuronal and vascular architecture, that may differ by brain region.

CONCLUSIONS

In general, the results of our meta-analysis are fairly intuitive. In terms of spatial smoothing, for discrete signals the optimal smoothing kernel should approximate the size of the underlying signal or evoked response. Based upon the fact that increases in blood flow and blood volume arise in gray matter, and that the spatial extent of gray matter differs between cortical and subcortical structures, the signal source would be expected to be more spatially extended for subcortical structures. Based upon the anatomical structure of cortical regions, the spatial extent of cortical activations would be expected to be in the order of 3–5 mm, suggesting a spatial smoothing of 6 mm would be the most efficient. In contradistinction, subcortical activations may be more spatially diffuse, engaging larger volumes of subcortical gray matter. The finding that subcortical activations were more powerfully detected using a higher degree of spatial smoothing is entirely

TABLE 4

Summary of Average Scores

	Z Scores	−ln (Euler)
Resampled voxel dimensions		
2 × 2 × 2 mm^3	5.26	6.59
3 × 3 × 3 mm^3	5.20	6.36
Spatial smoothing		
6 mm	5.35	5.74
10 mm	5.32	7.01
14 mm	5.02	6.67
Temporal smoothing		
4 s	5.60	8.47
8 s	4.86	4.48
Set of basis functions		
HRF (alone)	5.31	7.33
HRF and Temporal derivative	5.39	7.16
HRF and Temp and Dispersion deriv	4.99	5.17

consistent with the anatomical infrastructure expressing the hemodynamic responses. In addition, we found that after a correction for multiple comparisons had been imposed, a slightly larger spatial smoothing (10 mm) produced the most sensitive results for cortical regions. This is consistent with the nature of the correction, as a smaller smoothing kernel results in more comparisons across the volume.

In relation to temporal smoothing, one would generally anticipate that a smaller degree of temporal smoothing would give more efficient and sensitive tests. Again this is what we found and indeed the impact of temporal smoothing appeared to be greater than the other parameters we analyzed, in terms of percentage change of the uncorrected and corrected scores. The reason why less temporal smoothing gives a more sensitive analysis is because the most efficient characterization would involve prewhitening the data as opposed to smoothing it further. The reason that smoothing is employed is to ensure the robustness of the ensuing inferences by imposing a correlation structure on the time series. Although this renders the analysis less efficient, it protects against bias in the estimate of the standard error of the parameter estimates that enters as a result of misspecifying the form for these serial correlations (Friston *et al.*, submitted). Here, we show that applying a temporal smoothing as large as 8 s may, however, significantly decrease the power of the analysis.

In testing for the optimal basis set, we found that including the dispersion derivative decreased the sensitivity of the analysis. Both the HRF alone and the HRF with its temporal derivative engendered greater sensitivity than when the dispersion derivative was included.[3] While the HRF and the HRF with temporal derivative had comparable sensitivity, it may be more prudent to use the HRF with the temporal derivative in order to account for slight temporal shifts in the data (see also Aguirre *et al.*, 1997, and Rajapakse *et al.*, 1999, for alternative methods of modeling the hemodynamic response).

In terms of resampled voxel size, the smaller resampled voxel size did produce a significantly greater sensitivity, although the absolute measures of sensitivity changed only a small amount. The increase in sensitivity with 2-mm voxels is probably a result of the slight implicit smoothing in the sinc interpolation. All interpolations are effectively linear combinations of the local voxel values and can be thought of in terms of a spatial smoothing. Any resampling of data slightly smoothes it and therefore renders the analysis more sensitive. Here we used only sinc interpolation in resampling the voxel size. Simpler forms of interpolation may be used, but could result in a loss of information, in terms of resolution. A possible extension of this work would be to include multiple types of interpolation as a factor in the meta-analysis.

In summary, these results suggest optimal values for the analysis parameters of spatial smoothing, temporal smoothing, and resampled voxel size, and furthermore show that including only the temporal derivative with the HRF can provide flexibility in modeling event-related fMRI responses without compromising sensitivity. This paper presents an approach to assessing fMRI analysis parameters that can identify optimal parameters for the analysis of fMRI datasets. The equipment used to acquire the data and the specifications concerning the acquisition parameters may also affect the ultimate sensitivity of analyses, although we have not tested those factors here. While the specific values found to be optimal here may differ somewhat depending upon acquisition parameters and scanning equipment, the general trends found here (i.e., the decrease in sensitivity with a larger temporal smoothing kernel or the interaction between smoothing and brain region) are more likely to generalize, as these effects are based upon postacquisition parameter settings.

[3] It should be noted, however, that the dispersion derivative may be important for finding regions that have a different form or shape of hemodynamic response. The present meta-analysis only considered regions that evidenced suprathreshold clusters in all 36 analyses—any region that was significant in only one or a few sets of analyses was not considered here. Therefore, the dispersion derivative could still be very useful under certain circumstances (see also Rajapakse *et al.*, 1999, for related issues).

ACKNOWLEDGMENTS

J.B.H. was supported by funding from the National Science Foundation. C.B., A.P.H., and K.J.F. were supported by the Wellcome Trust. We thank Dr. G. R. Mangun for his support of this project.

REFERENCES

Adler, R. 1981. *The Geometry of Random Fields*. Wiley, New York.

Aguirre, G. K., Zarahn, E., and D'Esposito, M. 1997. Empirical analyses of BOLD fMRI statistics. II. Spatially smoothed data collected under null-hypothesis and experimental conditions. *Neuroimage* **5:**199–212.

Aguirre, G. K., Zarahn, E., and D'Esposito, M. 1998. The variability of human, BOLD hemodynamic responses. *Neuroimage* **8:**360–369.

Büchel, C., Morris, J., Dolan, R. D., and Friston, K. J. 1998. Brain systems mediating aversive conditioning: An event-related fMRI study. *Neuron* **20:**947–957.

Friston, K. J., Josephs, O., Rees, G., and Turner, R. 1998. Nonlinear event-related responses in fMRI. *Magnetic Resonance in Medicine* **39:**41–52.

Friston, K. J., Josephs, O., Zarahn, E., Holmes, A. P., Rouquettes, S., and Poline, J-B. *To Filter or Not to Filter: Bias and Efficiency in fMRI Time Series Analysis*, submitted.

Friston, K. J., Ashburner, J., Poline, J-B., Frith, C. D., Heather, J. D., & Frackowiak, R. S. J. 1995a. Spatial realignment and normalization of images. *Hum. Brain Mapp.* **2:**165–189.

Friston, K. J., Holmes, A. P., Poline, J-B., Grasby, P. J., Williams, S. C. R., and Frackowiak, R. S. J. 1995b. Analysis of fMRI time-series revisited. *Neuroimage* **2:**45–53.

Holmes, A. P., Josephs, O., Büchel, C., and Friston, K. J. 1997. Statistical modeling of low-frequency confounds in fMRI. *Proceeding of the 3rd International Conference of the Functional Mapping of the Human Brain*. S480.

Josephs, O., Turner, R., and Friston, K. J. 1997. Event-related fMRI. *Hum. Brain Mapp.* **5:**243–248.

Purdon, P. L., and Weisskoff, R. M. 1998. Effect of temporal autocorrelation due to physiological noise and stimulus paradigm on voxel-level false-positive rates in fMRI. *Hum. Brain Mapp.* **6:** 239–249.

Rajapakse, J. C., Kruggel, F., Maisog, J. M., and von Cramon, D. Y. 1998. Modeling hemodynamic response for analysis of functional MRI time-series. *Hum. Brain Mapp.* **6:**283–300.

Skudlarski, P., Constable, R. T., and Gore, J. C. 1999. ROC analysis of statistical methods used in functional MRI: Individual subjects. *Neuroimage* **9:**311–329.

Talairach, P., and Tournoux, J. 1988. *A Stereotactic Coplanar Atlas of the Human Brain*. Stuttgart, Thieme.

Thacker, N. A., Burton, E., Lacey, A. J., and Jackson, A. 1999. The effects of motion on parametric fMRI analysis techniques. *Physiol. Meas.* **20:**251–263.

Worsley, K. J. 1994. Local maxima and the expected Euler characteristic of excursion sets of X^2, F and T fields. *Adv. Appl. Prob.* **26:**12–42.

Worsley, K. J., and Friston, K. J. 1995. Analysis of fMRI time-series revisited—Again. *Neuroimage* **2:**173–181.

Zarahn, E., Aguirre, G. K., and D'Esposito, M. 1997. Empirical analyses of BOLD fMRI statistics. I. Spatially unsmoothed data collected under null-hypothesis conditions. *Neuroimage* **5:**179–97.